

A novel economical friendly treatment approach: Composite hydrogels

Nadher D Radhy*, Layth S Jasim

Department of Chemistry, College of Education, University of Al-Qadisiyah, Iraq

* Corresponding author's E-mail: n_education77@mail.ru

ABSTRACT

There are many chemical indicators of drinking water pollution. These include heavy metals, radioactive materials, inorganic chemicals, organic chemicals, disinfectants, and disinfectant additives. Common methods for removing these contaminants from aqueous solutions include chemical precipitation, membrane processes, ion exchange processes, biological processes, adsorption, and chemical reactions. Each of these methods has limitations in application. Many studies have been performed on the use of graphene in filters. Graphite oxide (GO) platelets were prepared using a modified Hummers method. By employing GO platelets, GO/poly (acrylic acid – maleic acid) superabsorbent composites were synthesized by a free radical polymerization of acrylic acid and maleic acid as a monomer, using N, N -methylenebisacrylamide as cross-linker and ammonium persulfate as initiator. The well-dispersed GO platelets in the polymer networks result in a significant improvement in absorbencies in distilled water solutions. The superabsorbent nanocomposite also exhibits a superior water-retention ability compared with the control under the same conditions. GO/P(AA-MA) composite was investigated using field emission scanning electron microscopy (FE-SEM) and Fourier transform infrared (FTIR); GO/P (AA-MA) composite is a highly effective absorbent of crystal violet (CV) and can be used to remove CV from aqueous solution. The kinetics of dye adsorption has been studied in terms of pseudo-first-order and pseudo-second-order rate expression. The results indicated that the adsorption process followed two models and demonstrated that intraparticle diffusion plays a significant role in the adsorption mechanism.

Keywords: Treatment, Drinking water pollution, Graphene oxide, Adsorption, Composite hydrogels.

Article type: Research Article.

INTRODUCTION

By the growth of urbanization and the rapid industrialization of cities, the problem of industrial pollution in the ecosystem has raised concerns in many parts of the world. Removal of these pollutants from water and sewage has received much attention due to strict laws in many countries to control water pollution. Dyes are organic colorant compounds that are extensively used in many different industrial fields such as textiles, tanning, paper, food, and cosmetics (Mahmood *et al.* 2005; Anastasi *et al.* 2010; Singh & Arora 2011; Banimahd Keivani 2018). Discharge of dyes into the environment can contaminate underground water and cause serious health and biological problems. Crystal violet (CV) is a common cationic dye, which belongs to the triphenylmethane group. This dye is widely used as a colorant, biological stain, and veterinary medicine. CV has been found to have harmful effects on humans and has been suspected of causing cancer (Zhang *et al.* 2014). Therefore, it is very important to separate and remove dyes from wastewater. There are many different methods for removal of dyes from water such as adsorption (Arulkumar *et al.* 2011), photodegradation (Tian *et al.* 2012), coagulation (Verma *et al.* 2012), ion exchange (Greluk & Hubicki 2010), and membrane filtration (Cheng *et al.* 2012). However, adsorption is the most attractive method because of its high efficiency, ease of operation, and cost-effectiveness. A wide range of different organic and inorganic adsorbents such as activated carbon (Mezohegyi *et al.* 2012),

clays (Bhatt *et al.* 2012), carbon nanotubes (Mishra *et al.* 2010), and polymeric materials (Yavuz *et al.* 2011; Shukla *et al.* 2012) have been prepared and used for dye adsorption. However, in many cases, the prepared adsorbents have a low surface area, low adsorption capacity, and weak mechanical strength in severe conditions. Therefore, it is still necessary to develop mechanically strong adsorbents with high efficiency. Polymeric hydrogels are very attractive for dye adsorption since water can easily diffuse through the hydrophilic polymer network, and dissolved dyes can interact strongly with numerous functional groups present in the structure of polymer chains. The adsorption of dyes strongly depends on the structure and composition of the hydrogels. Polymeric hydrogels with different compositions have been used for the adsorption of cationic and anionic dyes (Li *et al.* 2011a; Li *et al.* 2011b; Panic *et al.* 2013; Aljeboree & Alshirifi 2018). Hydrogels with negative charges in their structures are effective in the removal of cationic dyes, while positively charged hydrogels are appropriate for the removal of anionic dyes (Panic *et al.* 2013). Zwitterionic hydrogels can be used for both cationic and anionic dyes (Shukla *et al.* 2012). However, the weak mechanical strength of the hydrogels is one of their drawbacks that limits the application of hydrogels, especially for repeated cycles of adsorption. In many cases, hydrogels are filled with inorganic materials to improve their mechanical properties. Clays (Chang *et al.* 2010) and carbonaceous materials such as carbon nanotube (Chatterjee *et al.* 2010) and graphene (Zhang *et al.* 2011) have been used for this purpose. It was also found that the presence of inorganic materials increases the adsorption capacity of dyes (Metin *et al.* 2013). Graphene oxide (GO) is a carbonaceous material that has attracted much attention in recent years (Zhu *et al.* 2010; Chen *et al.* 2012). GO is produced by oxidation of graphite, which leads to introducing different oxygen-containing functional groups such as hydroxyl, epoxy, and carbonyl groups. These functional groups can interact with dye molecules through hydrogen bonds and electrostatic interactions. These properties make GO a good candidate for dye adsorption. Incorporating GO into hydrogels leads to the formation of nanocomposite adsorbents with high mechanical strength (Fan *et al.* 2013). The presence of GO not only improves the physical properties of hydrogel but also increases its adsorption capacity. Although it has been shown that GO itself and also polymeric hydrogels can be used as dye adsorbents (Liu *et al.* 2012), synthesis of GO-based nanocomposites can combine properties of both GO and hydrogels. As a result, adsorbents with high mechanical strength and adsorption capacity could be obtained. Although GO and its polymeric nanocomposites have been studied extensively in recent years, there are few reports in the field of GO–hydrogel nanocomposites for dye adsorption (Pourjavadi *et al.* 2013). Herein, we report the synthesis and characterization of a novel composite hydrogel containing GO. The composite has consisted of the hydrogel in which GO sheets. The polymeric network of the hydrogel is composed of acrylic acid and maleic acid. The synthesized composite was used as a dye adsorbent, and its ability for removal of CV was studied. The effect of different experimental conditions on dye adsorption was also investigated.

MATERIALS AND METHODS

Chemicals and materials

Natural graphite powders, potassium permanganate (KMnO₄), sodium nitrate (NaNO₃), concentrated sulfuric acid, hydrochloric acid, hydrogen peroxide (30%), acrylic acid (AA), maleic acid (MA), N, N'-methylene-bisacrylamide (MBA), ammonium persulfate (APS), crystal violet (CV) and sodium hydroxide were purchased from Kemiou Chemical Reagent Co, Ltd, China. All the reagents used were analytical grade pure with no further purification, and all the solutions were prepared with deionized water.

Preparation of GO

GO was prepared according to the modified Hummers method (Marcano *et al.* 2010). Briefly, 1.0 g of sodium nitrate was stirred with 1.0 g of natural graphite in an ice-water bath for 10 minutes. Once the mixture was well-mixed, 46 mL of sulfuric acid was added gradually into the mixture. The mixture was kept between the temperature ranges of 0 °C to 5 °C in the ice-water bath as a safety precaution. While maintaining vigorous agitation, 6.0 g of potassium permanganate was added into the suspension gradually. The rate of addition was controlled to prevent the temperature of the mixture from exceeding 20 °C. The mixture was kept mixing for a total of 2 hours, with the temperature of the ice-water bath kept at ≤ 5 °C. The ice-water bath was then removed, and the mixture was stirred overnight at room temperature. As the reaction progressed, the mixture gradually



thickened. After a night of stirring, the mixture became pasty, and it became brownish grey in color. Thereafter, 135 mL of deionized water was slowly stirred into the paste, and this resulted in violent effervescence and a temperature hike to 98 °C. A watch glass was used to minimize evaporation, and the level of the mixture was maintained at 250 mL with the periodical addition of deionized water for 1 hour. Subsequently, the heater was turned off, and the mixture was then left to cool for 1 hour to room temperature. Once completed, 10 mL of hydrogen peroxide (30%) was added dropwise to reduce the residual permanganate and manganese dioxide to colorless soluble manganese sulfate. After the filtration of the mixture, the residue was washed with 10% HCl solution four times and ultrapure water five times.

The product was dialyzed with deionized water for one week. Then, it was dried at 60 °C and stored for further use. To prepare fully exfoliated GO nanosheets with different concentration (3-6 mg mL⁻¹), different amount of GO powder was dispersed into 100 mL deionized water, followed by an ultrasonic for 30 min to form a yellow-brown stable GO solution.

Preparation of GO/P (AA-MA) composite

For the preparation of GO/P (AA-MA) composite, at first, 2 mL GO (3, 4, 5, and 6 mg mL⁻¹) water solution mixed with AA (0.08 mol), MA (0.02 mol), MBA (0.032-0.22 mmol) APS (0.015 g) were dissolved in double distilled water to the total volume of 10 mL. Then, the mixture was sonicated for 10 min and became homogenized were poured into a glass container, heated slowly to 55 °C (over about 10 min) under an N₂ atmosphere and kept at this temperature for two hours. After being cooled down to room temperature, the resulting hydrogel was immersed in the deionized water and washed in excess deionized water ten times to remove the soluble impurities in the hydrogel.

Characterization of hydrogel and composites

Fourier transform infrared spectroscopy (FT-IR)

FT-IR spectrometric (Shimadzu 8400S, Japan) analysis was used to characterize the chemical structure of the P (AA-MA) hydrogel and GO/P (AA-MA) composite. All samples were prepared as KBr Pellets and spectra in the frequency range (4000-400) cm⁻¹.

Field-Emission Scanning electron microscopy (FE-SEM)

The surface morphology of the composite and hydrogel were examined using Field-Emission scanning electron microscopy (FE-SEM) (Tescan MIRA3, Germany), followed by analyzing the GO/P(AA-MA) composites and P(AA-MA) hydrogel.re analyzed. The composite and hydrogel were coated with a thin layer of gold under reduced pressure, and their FE-SEM images were taken.

Preparation surface of composite

The surface of the composite in powder forms was washed with excessive amounts of distilled water. Several washings were performed to remove dust and soluble materials. The washed surface was then dried in an oven at 40 °C for a period of 6 hours and kept in airtight containers. The surface was then ground and sieved using a different mesh sieve (100-400 μm). The particle size of 100 μm was used for the surface in all experiments of this work.

Determination of Maximum Absorption (λ_{max})

To determine the maximum wavelength of the CV dye, the ultraviolet-visible absorption spectra of the dye solution (20 mg L⁻¹) was recorded within wavelengths of 200-800 nm. The maximum wavelength of the dye solution was determined from its highest absorption in the UV-Vis spectrum found at the wavelength λ_{max} CV = 591.0 nm (Fig. 1).

Calibration Curves of CV dye

Solutions of different concentrations of CV dye prepared by serial dilutions. Absorbance values of these solutions were measured at the selected λ_{max} (591.0 nm) value for dye and plotted against the concentration values CV (Fig. 2). The calibration curves in the concentration range that falls in the region of applicability of Beer-Lambert's law were employed.



Determination of the Optimum Amount of graphene oxide in the composite

The different weight ratio of the GO (3-6 mg) has been prepared in the composite. Then, we added a constant weight of 0.05 g of each ratio to a volume of 10 mL of the CV dye solution at 25 °C, put all the solutions in the shaker, and start stirring for 120 min. The end is the separation of the solutions by the centrifuge at 6000 rpm for 15 min and measurement of absorbance after adsorption using a UV-Visible spectrophotometer.

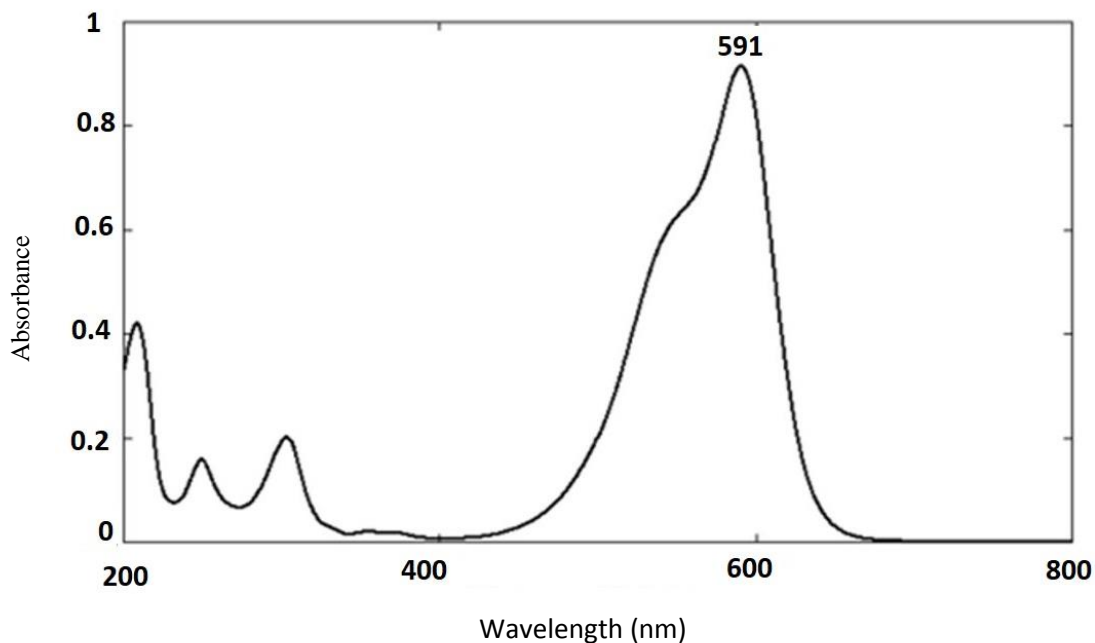


Fig. 1. UV-Visible absorption spectra.

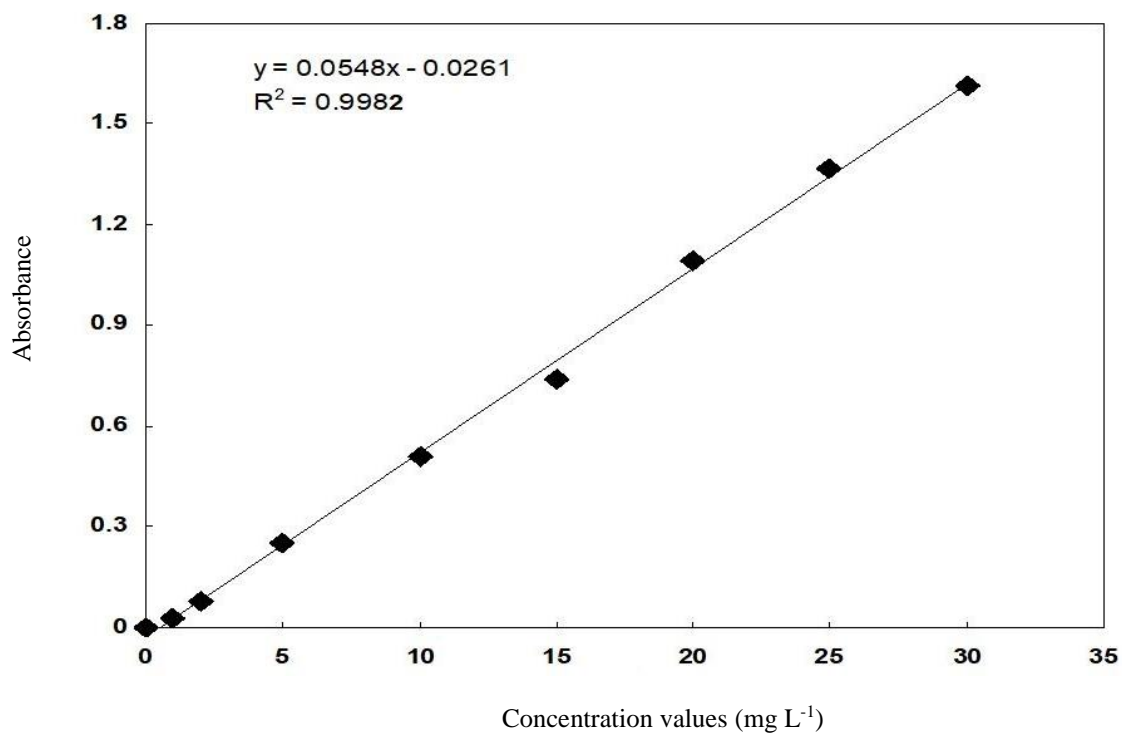


Fig. 2. Calibration curves of the CV dye.

Calculate the quantity adsorbed

The quantity of dye adsorbed was calculated according to the following equation:

$$\frac{x}{m} = \frac{V(C_o - C_e)}{m} \quad (1)$$

where x : the quantity adsorbed; m : weight of adsorbent (g); C_o: initial concentration (mg L⁻¹); C_e: equilibrium concentration (mg L⁻¹); V : volume of solution (L).

Kinetic Studies

The effect of contact time was determined by adding 0.03 g of adsorbent into 10 mL dye solution, with initial concentration (500 mg L⁻¹) under shaking. The temperature of the solution was held constant at 25 °C with a thermostatic shaker. After different time intervals, the solutions were centrifuged, and volumes of 3 mL supernatant were taken for spectrophotometric measurements of dye content.

Swelling studies of composite

The swelling properties of the composite hydrogel were performed by gravimetric analysis. Briefly, 0.1g of dry composite hydrogel was immersed in 500 mL of the swelling medium pH (7 and 1) at 25 °C. At regular time intervals, the gels were removed from the medium, the weight of the swollen composite hydrogel was determined after the removal of the surface water through blotting with filter paper. The measurements were continued until the weight of hydrogels reached a constant value. The swelling ratio (SR) was calculated by the following:

$$SR = \frac{(W_t - W_d)}{W_d} \quad (2)$$

where W_t is the mass of the swollen hydrogels at t, and W_d is the initial mass of dry hydrogel.

RESULTS AND DISCUSSION

Characterization of graphene oxide

The FTIR spectrum in Fig. 3 of pristine graphite exhibits no characteristic peak for the discernible functional groups. It only displays four peaks at approximately 1605, 3444, 3010, and 1100 cm⁻¹ attributed to the skeletal vibrations from graphite domains (the sp² aromatic C=C) and the vibration of adsorbed water molecules (the O-H stretching), and correspond to the presence of a C-H and C-H bending bond respectively. After treating by oxidizing agents, the oxygenated graphene sheet could display a series of different absorption bands or characteristics peaks ranging from 900 to 3500 cm⁻¹. The O-H stretches vibration at 3400 cm⁻¹ (hydroxyl), the C=O (carboxyl and carbonyl) at 1720 cm⁻¹, the residual sp² skeletal vibration of un-oxidized graphitic fields (C=C) at 1620 cm⁻¹, the C-O (carboxyl, C-OH) at 1220 cm⁻¹, the C-O (epoxy) groups at 1226 cm⁻¹, the C-O (ring) at 1060 cm⁻¹ and C-H at 2950 cm⁻¹ (Alwan *et al.* 2018).

The FTIR spectra of the P (AA-MA) hydrogel the presence ν(O-H, N-H) overlap bonds at 3000-3440 cm⁻¹ and C-H stretching at 2890 cm⁻¹ and also C=O stretching vibration absorption bonds in carboxylic groups at 1720 cm⁻¹, but C=O stretching vibration absorption bonds in amide groups at 1650 cm⁻¹, O-H bending for -COOH at 1400 cm⁻¹, and C-O bending at 1560 cm⁻¹. However, the FTIR for GO/P(AA-MA) showed the shift of the groups' bands reveals the interactions between the carboxylic groups on P(AA-MA) and GO platelets (Lee *et al.* 2014) given in Fig. 4.

FE-SEM, a common technique was used to identify the surface morphology of graphite, GO, P (AA-MA), and GO/P(AA-MA). FE-SEM images of graphite sheets explain a closely-aligned layered structure and be stack as layer thick. It also exhibits a flaky appearance for the strong sp² carbon to carbon bonding in the plane. After oxidation, the FE-SEM image of GO nanosheets indicates a wavy frizzy appearance, the surface is bristly, and the edges of the sheets are foggy. At higher concentrations, the surface of GO shows coarse carpet, which can due to the link of residual water molecules, carboxyl, and hydroxyl groups with the sheets (Aunkor *et al.* 2015) given in Figs. 5 and 6. The FE-SEM images of P (AA-MA) hydrogel and GO/P (AA-MA) composite samples are shown in Figs. 7-8. The P (AA-MA) hydrogel shows a smooth and neat surface morphology, and after the introduction of GO platelets into the P (AA-MA) hydrogel network, the surface morphology of the GO/P (AA-MA) composite sample becomes rougher, and the GO/P (AA-MA) composite sample shows an irregular, plat-like structure. The



formation of such a structure of GO/P (AA-MA) may be induced by a plate-like layer of GO platelets. In addition, it can be seen that the GO platelets are well dispersed throughout the polymer matrix as individual platelets, and no obvious aggregation was observed. Such a good dispersion of GO platelets into the polymer matrix has also been achieved in other polar polymer GO systems (Wan *et al.* 2016).

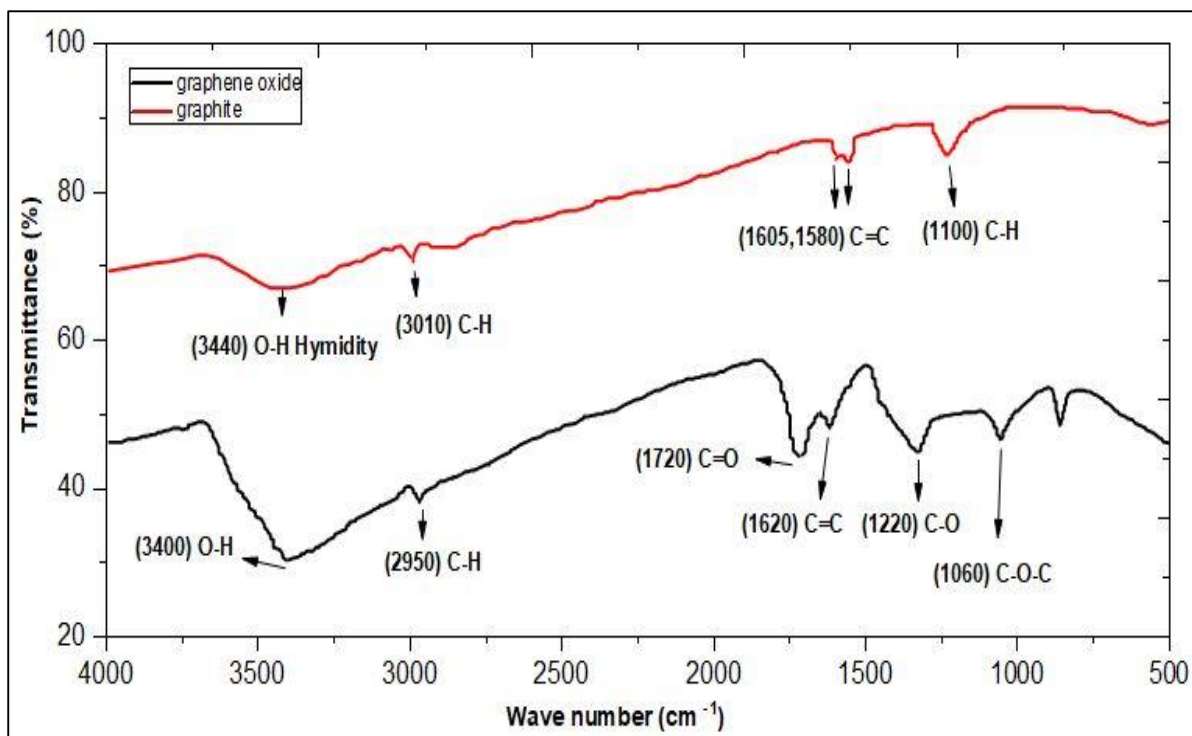


Fig. 3. FTIR spectra of Graphite and Graphene Oxide.

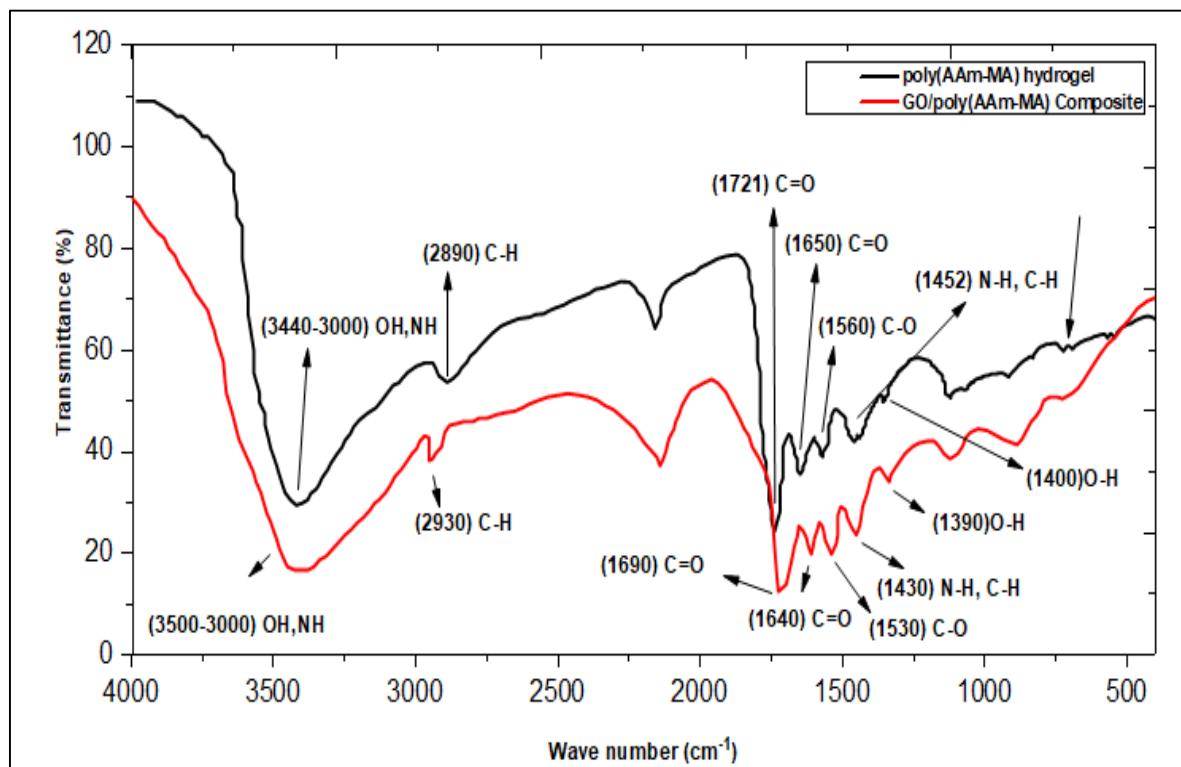


Fig. 4. FTIR spectra of P (AA-MA) and GO/P (AA-MA).

Adsorption Kinetic Models

To determine the equilibrium time for the maximum uptake of the dye, the adsorption of crystal violet on GO/P (AA-MA) composite was studied as a function of contact time, and the results are shown in Fig. 9. It can be concluded that the rate of dye uptake on GO/P (AA-MA) composite is higher during the initial stages and gradually decrease and become almost constant after a period of 120 min, which could be due to the high number of available adsorption sites at the beginning of the adsorption process, which then later became saturated.

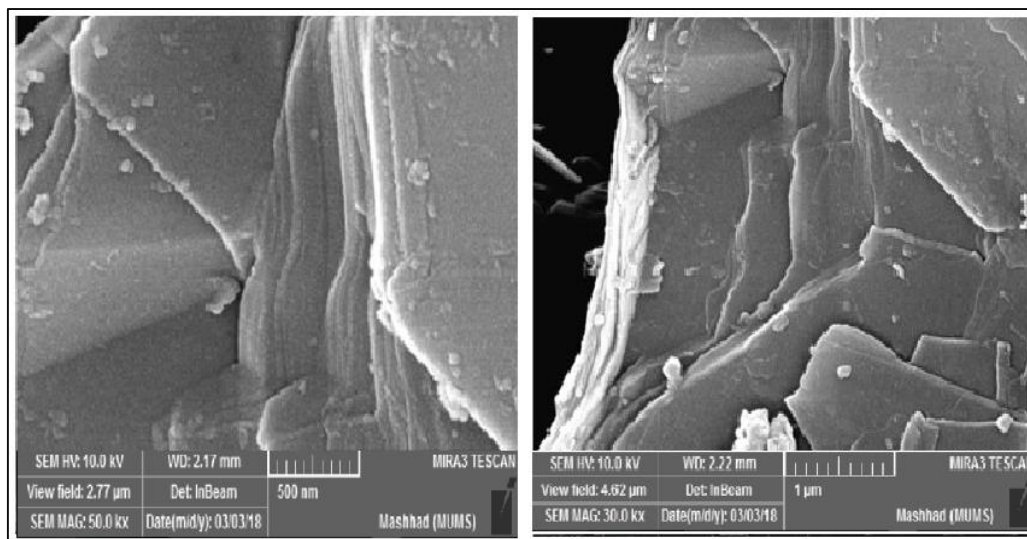


Fig. 5. FE-SEM images of Graphite.

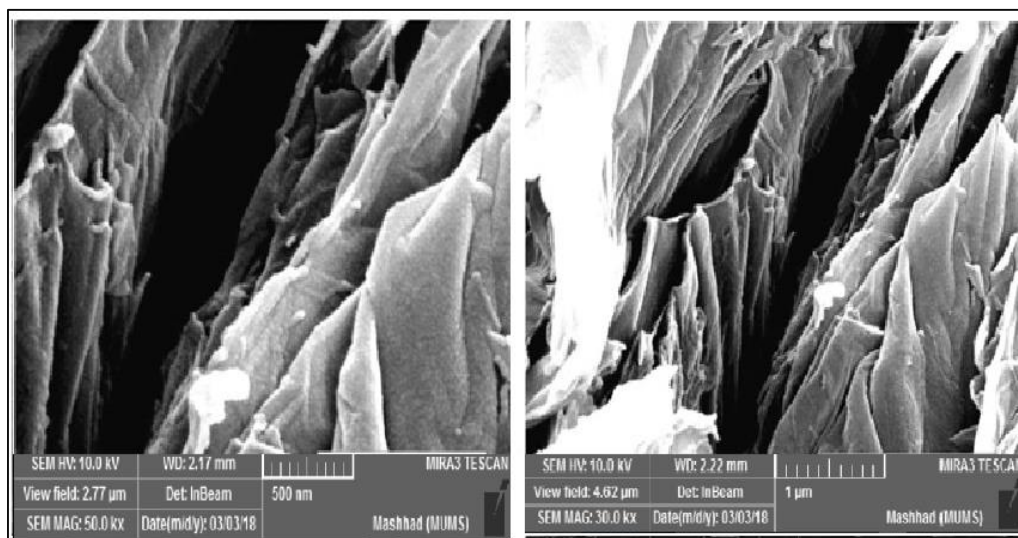


Fig. 6. FE-SEM images of GO.

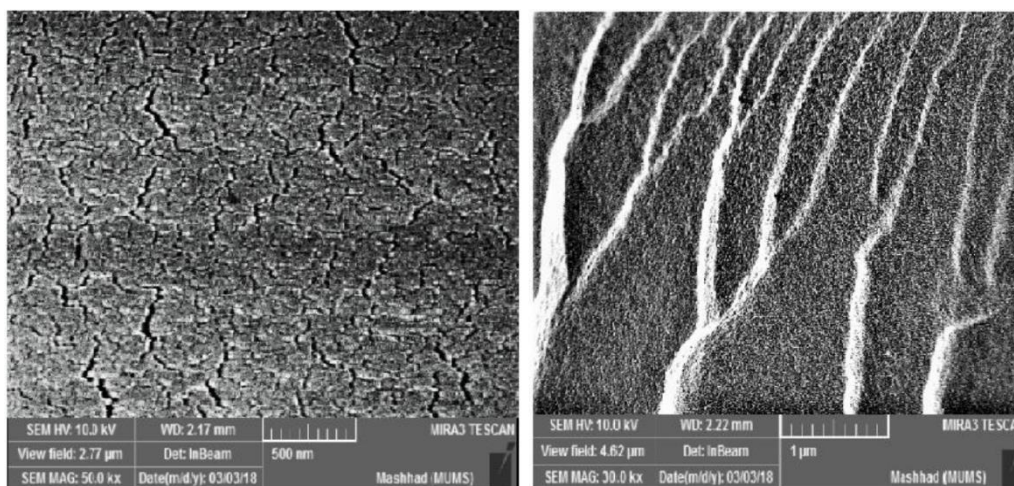


Fig. 7. FE-SEM images of P (AA-MA) hydrogel.

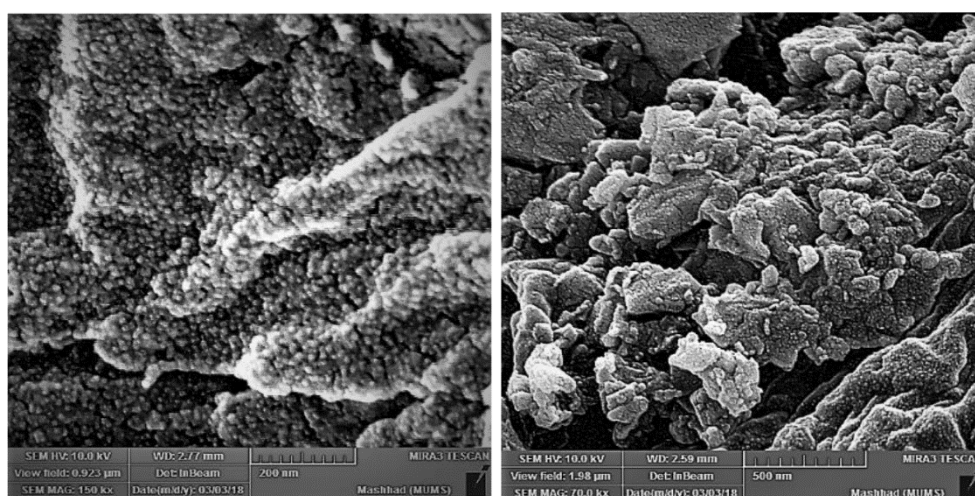


Fig. 8. FE-SEM images of GO/P (AA-MA) composite.

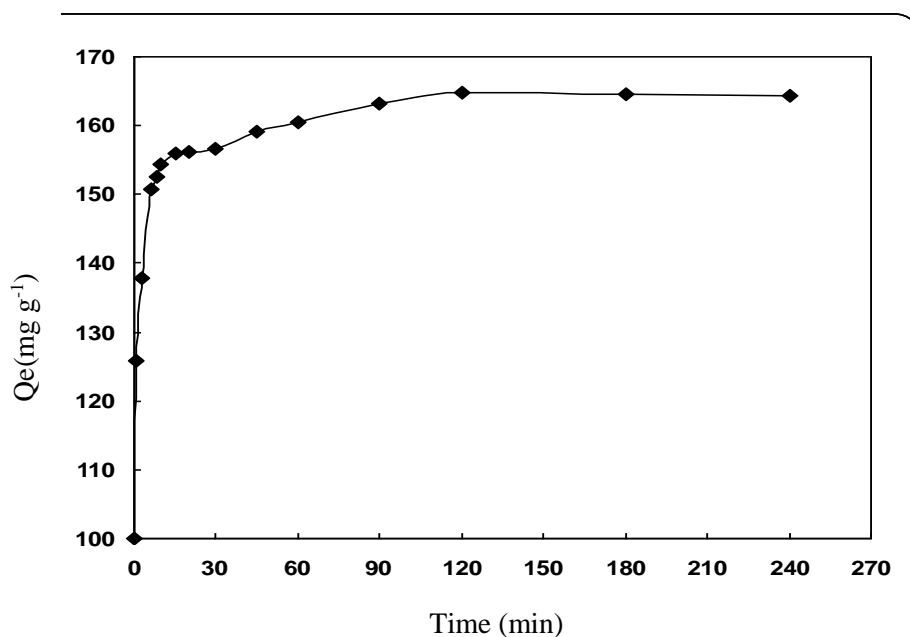


Fig. 9. The effect of contact time on adsorption capacity.

Several kinetic models are available to examine the controlling mechanism of the adsorption process and to test the experimental data. The rate constants of the dye removal from the solution by GO/P (AA-MA) composite were determined using first order and pseudo-second-order equations.

The Lagergren first-order rate equation was used to fit the experimental results. The linear form of the Lagergren equation is:

$$\ln(q_e - q_t) = \ln q_e - k_1 t \quad (3)$$

where q_e (mg g^{-1}) is the equilibrium sorption capacity, and q_t (mg g^{-1}) is the amount of dye adsorbed at time t (min). Values of k_1 for CV-GO/P(AA-MA) composite system was obtained from the slope of the plot of $\ln(q_e - q_t)$ vs. t (Fig. 10). The adsorption kinetic parameters from Fig. 11 are indicated in Table 1.

The adsorption data were also analyzed in terms of a pseudo-second-order mechanism. The linear form of the equation is:

$$\frac{t}{q_t} = \frac{1}{k_2 q_e^2} + \left(\frac{1}{q_e}\right) t \quad (4)$$

where k_2 ($\text{g mg}^{-1} \text{min}^{-2}$) is the rate constant of the pseudo-second-order adsorption. If the initial adsorption rate is $h = k_2 q_e^2$. Then equation 4 becomes:

$$\frac{t}{q_t} = \frac{1}{h} + \left(\frac{1}{q_e}\right) t \quad (5)$$

By plotting t/q_t versus t , Fig. 10, a straight line could be obtained, and q_e , k_2 , and h can be calculated. The adsorption kinetic parameters from Fig. 11 are listed in Table 1.

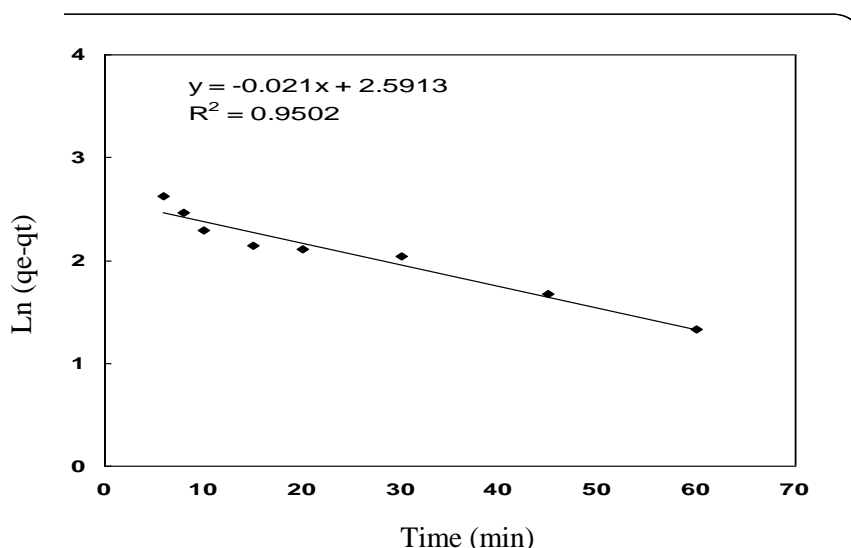


Fig. 10. Pseudo-first order kinetics for adsorption CV.

The applicability of the Lagergren and pseudo-second-order models can be examined by linear plots of $\ln(q_e - q_t)$ vs. t and t/q_t vs. t , respectively, as shown in Figs. 10-11, respectively. To quantify the applicability of each model, the correlation coefficient, R^2 , was calculated from these plots. The correlation coefficient, R^2 , shows that the pseudo-second-order model fits the experimental data slightly better than the pseudo-first-order. This fact indicates that intra-particle diffusion is the rate-controlling step. The mechanism of dye adsorption on the textile materials, which may involve the following three steps: (i) diffusion of dye molecules through the solution to the surface of adsorbent; (ii) adsorption of dye molecules on the surface of the materials through the molecular interactions; (iii) diffusion of dye molecules from the surface into the interior of the adsorbent molecules. The second step of the adsorption of dye on the materials is dependent on the nature of the dye molecules, such as anionic or cationic structures. Due to the negatively charged characteristics of GO/P (AA-MA) composite in aqueous media, the cationic dye should be adsorbed more rapidly than anionic dye. The results obtained here indicate the effect of columbic interactions between the adsorbent and dye.

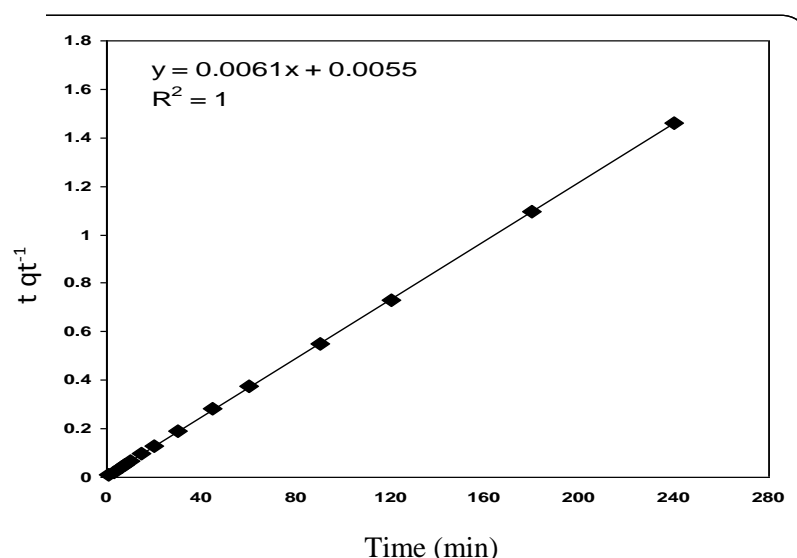


Fig. 11. Pseudo-second order kinetics for adsorption of CV.

Table 1. Adsorption kinetic parameters of CV on GO/P(AA-MA) composite.

| Dye | Pseudo- first order | | | Pseudo- second order | | | |
|----------------|--------------------------------|---------------------------------|-------|--|---------------------------------|-------|--|
| | k_1 (min^{-1}) | q_e (mg g^{-1}) | R^2 | K_2 ($\text{g. mg}^{-1}.\text{min}^{-1}$) | q_e (mg g^{-1}) | R^2 | h ($\text{mg. g}^{-1}.\text{min}^{-1}$) |
| Crystal Violet | 21×10^{-3} | 13.347 | 0.950 | 6.76×10^{-3} | 163.934 | 1 | 181.818 |

Swelling studies

The swelling ratio of the GO / P (AA-MA) was investigated for pH functions 7.0 and 1.0 because of its importance in the field of hydrogel applications such as adsorption. The results showed the extent of dependence the percentage of swelling on the pH function is very high (Fig. 12). It is observed that swelling rates are high at pH = 7.0 in comparison with pH = 1.0. This is due to the presence of hydrophilic groups in the chemical structure of the composite such as COOH, OH, C = O, pH = 7.0, which attributed to carboxyl groups on the composite became ionized but showed low swelling at acidic pH = 1.0. It is due to a high content of carboxylic acid groups that remain un-ionized at this pH, while the degree of swelling increases as the pH of medium elevates due to the availability of more carboxyl groups for ionization. As a result, electrostatic repulsion increases along the chain, which causes an expansion of the chain. After confirming the swelling effect at low and high pH, we were further interested to see the swelling as a function of crosslinking agents' concentration. Swelling decreases with increasing concentrations of cross-linker due to the increase in the degree of cross-linking between polymer chains, which prevents their expansion.

CONCLUSION

GO/P (AA-MA) composites were synthesized via a free radical polymerization using GO platelets. Our results show that the incorporation of GO platelets into the polymer network leads to a remarkable improvement in the absorbencies of the resulting superabsorbent composite in distilled water solution, which may be due to the fact that the good dispersion of GO platelets in the polymer matrix and in turn the formation of a more intact polymeric network structure, and then the network has additional space to allow more water to be held. The GO/P(AA-MA) composites could be employed as adsorbents in wastewater treatment for the removal of crystal violet dye. The process of adsorption is relatively fast, and the kinetic adsorption data fitted well to the second-order kinetic model, indicating an intra-particle diffusion mechanism.

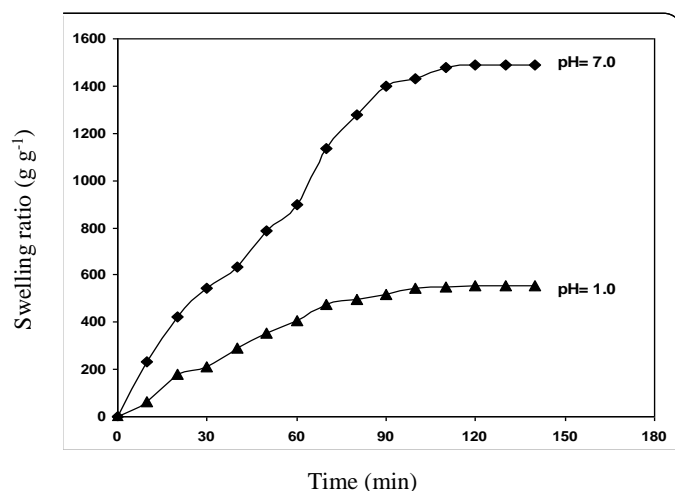


Fig. 12. Swelling ratio of GO P (AA-MA) composite hydrogels at 25 °C.

REFERENCES

- Aljeboree, AM & Alshirifi, AN 2018, Adsorption of Pharmaceuticals as emerging contaminants from aqueous solutions on to friendly surfaces such as activated carbon: A review. *Journal of Pharmaceutical Sciences and Research*, 10: 2252-2257.
- Alwan, SH, Alshamsi, HAH & Jasim, LS 2018, Rhodamine B removal on A-rGO/cobalt oxide nanoparticles composite by adsorption from contaminated water. *Journal of Molecular Structure*, 1161: 356-365.
- Anastasi, A, Prigione, V & Varese, GC 2010, Industrial dye degradation and detoxification by basidiomycetes belonging to different eco-physiological groups. *Journal of Hazardous Materials*, 177: 260-267.
- Arulkumar, M, Sathishkumar, P & Palvannan, T 2011, Optimization of Orange G dye adsorption by activated carbon of *Thespesia populnea* pods using response surface methodology. *Journal of Hazardous Materials*, 186: 827-834.
- Aunkor, MTH, Mahbulbul, IM, Saidur, R & Metselaar, HSC 2015, Deoxygenation of graphene oxide using household baking soda as a reducing agent: A green approach. *RSC Advances*, 5: 70461-70472.
- Banimahd Keivani, M 2018, Removal of brilliant blue pollution from the environment using nano polyaniline hazelnut skin composite and evaluation of effective parameters. *Caspian Journal of Environmental Sciences*, 16: 249-258.
- Bhatt, AS, Sakaria, PL, Vasudevan, M, Pawar, RR, Sudheesh, N, Bajaj, HC & Mody, HM 2012, Adsorption of an anionic dye from aqueous medium by organoclays: equilibrium modeling, kinetic and thermodynamic exploration. *RSC Advances*, 2: 8663-8671.
- Chang, CW, Van Spreeuwel, A, Zhang, C & Varghese, S 2010, PEG/clay nanocomposite hydrogel: A mechanically robust tissue engineering scaffold. *Soft Matter*, 6: 5157-5164.
- Chatterjee, S, Lee, MW & Woo, SH 2010, Adsorption of congo red by chitosan hydrogel beads impregnated with carbon nanotubes. *Bioresource Technology*, 101: 1800-1806.
- Chen, D, Feng, H & Li, J 2012, Graphene oxide: Preparation, functionalization, and electrochemical applications. *Chemical Reviews*, 112: 6027-6053.
- Cheng, S, Oatley, DL, Williams, PM & Wright, CJ 2012, Characterisation and application of a novel positively charged nanofiltration membrane for the treatment of textile industry wastewaters. *Water Research*, 46: 33-42.
- Fan, J, Shi, Z, Lian, M, Li, H & Yin, J 2013, Mechanically strong graphene oxide/sodium alginate/polyacrylamide nanocomposite hydrogel with improved dye adsorption capacity. *Journal of Materials Chemistry A*, 1: 7433-7443.
- Greluk, M & Hubicki, Z 2010, Kinetics, isotherm and thermodynamic studies of Reactive Black 5 removal by acid acrylic resins. *Chemical Engineering Journal*, 162: 919-926.
- Lee, S, Lee, H, Sim, JH & Sohn, D 2014, Graphene oxide/poly (acrylic acid) hydrogel by γ -ray pre-irradiation on graphene oxide surface. *Macromolecular Research*, 22: 165-172.

- Li, S, Liu, X, Huang, W, Li, W, Xia, X Yan, S & Yu, J 2011a, Magnetically assisted removal and separation of cationic dyes from aqueous solution by magnetic nanocomposite hydrogels. *Polymers for Advanced Technologies*, 22: 2439-2447.
- Li, S, Zhang, H, Feng, J, Xu, R & Liu, X 2011b, Facile preparation of poly (acrylic acid–acrylamide) hydrogels by frontal polymerization and their use in removal of cationic dyes from aqueous solution. *Desalination*, 280: 95-102.
- Liu, F, Chung, S, Oh, G & Seo, TS 2012, Three-dimensional graphene oxide nanostructure for fast and efficient water-soluble dye removal. *ACS Applied Materials & Interfaces*, 4: 922-927.
- Mahmood, Q, Zheng, P, Islam, E, Hayat, Y, Hassan, MJ, Jilani, G & Jin, RC 2005, Lab scale studies on water hyacinth (*Eichhornia crassipes* Martens Solms) for biotreatment of textile wastewater. *Caspian Journal of Environmental Sciences*, 3: 83-88.
- Marcano, DC, Kosynkin, DV, Berlin, JM, Sinitskii, A, Sun, Z, Slesarev, A, Alemany, LB, Lu, W & Tour, JM 2010, Improved synthesis of graphene oxide. *ACS Nano*, 4: 4806-4814.
- Metin, AU, Çiftçi, H & Alver, E 2013, Efficient removal of acidic dye using low-cost biocomposite beads. *Industrial & Engineering Chemistry Research*, 52: 10569-10581.
- Mezohegyi, G, van der Zee, FP, Font, J, Fortuny, A & Fabregat, A 2012, Towards advanced aqueous dye removal processes: A short review on the versatile role of activated carbon. *Journal of Environmental Management*, 102: 148-164.
- Mishra, AK, Arockiadoss, T & Ramaprabhu, S 2010, Study of removal of azo dye by functionalized multi walled carbon nanotubes. *Chemical Engineering Journal*, 162: 1026-1034.
- Panic, VV, Madzarevic, ZP, Volkov-Husovic, T & Velickovic, SJ 2013, Poly (methacrylic acid) based hydrogels as sorbents for removal of cationic dye basic yellow 28: Kinetics, equilibrium study and image analysis. *Chemical Engineering Journal*, 217: 192-204.
- Pourjavadi, A, Hosseini, SH, Seidi, F & Soleyman, R 2013, Magnetic removal of crystal violet from aqueous solutions using polysaccharide-based magnetic nanocomposite hydrogels. *Polymer International*, 62: 1038-1044.
- Singh, K & Arora, S 2011, Removal of synthetic textile dyes from wastewaters: A critical review on present treatment technologies. *Critical Reviews in Environmental Science and Technology*, 41: 807-878.
- Shukla, NB, Rattan, S & Madras, G 2012, Swelling and dye-adsorption characteristics of an amphoteric superabsorbent polymer. *Industrial & Engineering Chemistry Research*, 51: 14941-14948.
- Tian, C, Zhang, Q, Wu, A, Jiang, M, Liang, Z, Jiang, B & Fu, H 2012, Cost-effective large-scale synthesis of ZnO photocatalyst with excellent performance for dye photodegradation. *Chemical Communications*, 48: 2858-2860.
- Verma, AK, Dash, RR & Bhunia, P 2012, A review on chemical coagulation/flocculation technologies for removal of colour from textile wastewaters. *Journal of Environmental Management*, 93: 154-168.
- Wan, S, Hu, H, Peng, J, Li, Y, Fan, Y, Jiang, L & Cheng, Q 2016, Nacre-inspired integrated strong and tough reduced graphene oxide–poly (acrylic acid) nanocomposites. *Nanoscale*, 8: 5649-5656.
- Yavuz, E, Bayramoğlu, G, Arica, MY & Senkal, BF 2011, Preparation of poly (acrylic acid) containing core-shell type resin for removal of basic dyes. *Journal of Chemical Technology & Biotechnology*, 86: 699-705.
- Zhang, L, Wang, Z, Xu, C, Li, Y, Gao, J, Wang, W & Liu, Y 2011, High strength graphene oxide/polyvinyl alcohol composite hydrogels. *Journal of Materials Chemistry*, 21: 10399-10406.
- Zhang, Q, Zhang, T, He, T & Chen, L 2014, Removal of crystal violet by clay/PNIPAm nanocomposite hydrogels with various clay contents. *Applied Clay Science*, 90: 1-5.
- Zhu, Y, Murali, S, Cai, W, Li, X, Suk, JW, Potts, JR & Ruoff, RS 2010, Graphene and graphene oxide: Synthesis, properties, and applications. *Advanced Materials*, 22: 3906-3924.

Bibliographic information of this paper for citing:

Radhy, N, D, Jasim, L, S 2021, A novel economical friendly treatment approach: Composite hydrogels. *Caspian Journal of Environmental Sciences*, 19: 841-852

Copyright © 2021

Caspian Journal of Environmental Sciences, Vol. 19 No. 5 pp. 841-852
DOI: 10.22124/CJES.2021.5233



Received: May 10, 2021 Accepted: Aug. 26, 2021
© The Author(s)

Publisher: University of Guilan, Iran